https://doi.org/10.5194/bg-2019-323
Preprint. Discussion started: 30 September 2019

Biogeosciences Discussions
Open Access
EGU

Trace elements in mussel shells from the Brazos River, Texas: environmental and biological control

Authors: Alexander A. VanPlantinga[1] and Ethan L. Grossman[1]
[1]Department of Geology and Geophysics, Texas A&M University, College Station, Texas, USA 77843-3115

Abstract. In sclerochronology, understanding the drivers of shell chemistry is necessary in order to use shells to reconstruct environmental conditions. We measured the Mg, Ca, Sr, Ba, and Mn contents in water samples and in the shells of two freshwater mussels (*Amblema plicata* and *Cyrtonaias tampicoensis)* from the Brazos River, Texas to test their reliability as environmental archives. Shells were analyzed along growth increments using age models established with stable and clumped isotopes. Shells were also examined with cathodoluminescence (CL) microscopy to map Mn/Ca distribution patterns. Sr/Ca correlated with Mn/Ca, while Mg/Ca and Ba/Ca showed no clear trends. Mn/Ca correlated inversely with the log of river discharge. Because dissolved and inorganic particulate sources of manganese are low during low flow, peak Mn/Ca values may come from elevated feeding or metabolic rates. Shell Mn/Ca values were used to reconstruct river discharge patterns, which, to our knowledge, has previously only been performed with shell chemistry using oxygen isotopes.

1 Introduction

Sclerochronology is the study of the physical and chemical properties of invertebrate hard parts. There is great potential for using mollusks to reconstruct environmental conditions in the present and in the geologic past, but problems remain in understanding the relationship between mollusk shell chemistry and the ambient environment (Immenhauser et al., 2016). For example, shell Sr/Ca can record temperature as a reflection of mollusk metabolic response to seasonal temperature variation opposite what is thermodynamically predicted for aragonite (Wheeler, 1992; Gillikin et al., 2005; Carré et al., 2006; Sosdian et al., 2006; Gentry et al., 2008). Shell Mg/Ca can record temperature (Freitas et al., 2006), and shell Ba/Ca sometimes correlates with diatom primary productivity (Vander Putten et al., 2000; Lazareth et al., 2003), but it can also be controlled by growth rate (Izumida et al., 2011). Mollusk soft tissue reflects variations in metal bioaccumulation by organ and by element (Arafin and Bendell Young, 2000; Chale, 2002; Ravera et al., 2003; Silva et al., 2006; Bellotto and Mieckeley, 2007). Soft tissue bioaccumulation can in turn elucidate pathways to shell bioaccumulation (Puente et al., 1996; Bilos et al, 1998; Langlet et al., 2007).

https://doi.org/10.5194/bg-2019-323
Preprint. Discussion started: 30 September 2019

Untangling the physical, chemical, and biological factors involved in sclerochronology will improve the utility of mollusk shells as environmental archives (Vander Putten et al., 2000).

Studies of mollusk shell Mn/Ca have highlighted chemical, physical, and biological pathways of environmental manganese, providing insight into mollusk physiology, ecosystems, food webs, and human impacts such as soil erosion, eutrophication, and hypoxia (Risk et al., 2010; Langlet et al., 2007; Jacob et al., 2008; Zhao et al., 2016; Zhao et al., 2017a). Aquatic manganese, whether dissolved or particulate, is controlled by redox conditions (pH and DO), which are in turn controlled by nutrient flux (Langlet et al., 2007), microbial oxidation (Sunda and Huntsman, 1990), and physical factors such as wind and water currents and photoreduction (Sunda and Huntsman, 1994). Manganese can be incorporated in mollusk shells via suspended organic particle ingestion (Bilos et al., 1998; Vander Putten et al., 2000; Lazareth et al., 2003; Langlet et al., 2007). Dissolved Mn^{2+} is the most bioavailable form of manganese (Campbell, 1995), and experimental studies using Mn-spiked water have shown the direct influence of dissolved Mn on shell Mn (Jeffree et al., 1995; Hawkes et al., 1996; Markich et al., 2002; Langlet et al., 2006; Lartaud et al., 2010). Naturally dissolved Mn variation has been demonstrated to influence shell Mn/Ca in several studies (Frietas et al., 2006; Barats et al., 2008; Zhao et al., 2017a). Nevertheless, little is known about the spatial and temporal variation of dissolved and inorganic and organic forms of manganese, including the chemistry of river colloids, sediment porewater, and phytoplankton.

While trace element studies of marine bivalves are common, trace element studies of freshwater mussels are uncommon despite the fact that freshwater mussels are threatened worldwide by anthropogenic nutrient influxes and water impoundment (Lydeard et al., 2004; Richter et al., 1997). Studies of freshwater mussel trace elements have highlighted the relationship between shell metal/Ca (Me/Ca) values and water Me/Ca values (Carroll and Romanek, 2008; Bolotov et al., 2015; Geeza et al., 2018), and relationships between Me/Ca and physical factors such as river discharge (Risk et al., 2010) and nutrient pollution (Zhao et al., 2017a).

This study explores relationships between the Brazos River physical and chemical parameters and the Mg, Sr, Ba, and Mn contents of freshwater mussel shells during the drought period of 2013. This work utilizes the oxygen isotope sclerochronology from VanPlantinga and Grossman (2018) established with the aid of clumped isotopes. This approach allows for the study of a challenging and dynamic environment, a subtropical regulated river where the mussel shell isotope record cannot be tied to seasonal patterns as easily as in temperate, tropical, or

https://doi.org/10.5194/bg-2019-323
Preprint. Discussion started: 30 September 2019

marine environments. Building on the water and shell isotope data, the present study focuses on trace metals and their relation to river nutrients. Although the shell Sr/Ca-temperature relationship was expected, the inverse Mn/Ca-discharge relationship indicates that river flow controls the bioavailability of manganese. Below we explore the basis for this observation and recommend further research on river manganese flux.

2 Methods

2.1 Setting, water sampling and analysis

This study focuses on the middle run of the Brazos River near College Station, Texas (near the USGS gage 08108700 in Bryan, Texas) about 210 km north of its estuary in the Gulf of Mexico (Figure 1). Water impoundment near this study site negatively impacts mussel diversity (Randklev et al., 2013; Tsakiris and Randklev, 2016) in the Brazos River. The Brazos flows southeast through a semi-arid to semi-humid climate characterized by hot summers and mild winters, averaging 29˚C and 13˚C, respectively (Nielsen-Gammon, 2011). Average annual rainfall in College Station is 100 cm and historically peaks in late-spring and mid-fall. About 240 km upstream of the study site is Lake Whitney, dammed for hydropower and flood control. About 30 km upstream of the study site is the confluence with the Little River, the largest Brazos tributary, receiving flows from Lake Belton, Stillhouse Hollow Lake, and Granger Lake, all dammed reservoirs. The Brazos is noted for high turbidity during times of high discharge, and, conversely, high suspended chlorophyll concentration and high rates of water column primary productivity at low flow (Roach et al., 2014).

From January 2012 through July 2013, weekly temperature, pH measurements, and water samples were collected from the Brazos River at the Highway 60 bridge between Brazos and Burleson counties (VanPlantinga et al., 2017). Water samples were measured for $\delta^{18}O$ and δD using a Picarro L2120i cavity ringdown spectrometer at the Stable Isotope Geoscience Facility at Texas A&M University. Calibration procedures, water $\delta^{18}O$, and temperature values are given in VanPlantinga et al. (2017). Discharge data for the Brazos River at Highway 21 near College Station (USGS 08108700) were obtained online from http://waterdata.usgs.gov/tx.

2.2 Shell samples and analyses

On August 9, 2013, four specimens each of *Amblema plicata* and *Cyrtonaias tampicoensis* were collected live from the Brazos River near the Highway 60 bridge, from the sandy river bed shallower than 2 m depth. Mussels were frozen, then shucked. Their shells were scrubbed, sonicated in water, and dried.

https://doi.org/10.5194/bg-2019-323
Preprint. Discussion started: 30 September 2019

One specimen each of modern young adult *A. plicata* (labelled 3R5) and *C. tampicoensis* (TP3) were randomly selected and analyzed. Based on stable and clumped isotope analyses, the shells are estimated to be 3-4 years old (VanPlantinga and Grossman, 2018). Specimens were sectioned, broken in two, and epoxied to glass slides. Shell powder samples were collected with a New Wave Micromill using a 0.5 mm drill bit following the methods of Dettman and Lohmann (1995). Two transects were sampled in each shell: one across the ventral margin region (or VM, also referred to as the outer nacreous layer or ONL), and one across the INL region (inner nacreous layer) as shown in Figure 2. Sample intervals were between 60 and 140 μm, with generally shorter spacing for INL than ONL. About 60 μg per sample were reacted in a Kiel IV carbonate instrument with phosphoric acid (specific gravity ≈ 1.925 g/cm^3) and the CO_2 analyzed on a Thermo Finnigan MAT253 mass spectrometer in the Stable Isotope Geosciences Facility at Texas A&M University. Average analytical precision was 0.05‰ for $\delta^{18}O$ and 0.03‰ for $\delta^{13}C$.

For ICP-MS analysis, 20-160 μg of powder were dissolved in 2 mL of 2% nitric acid solution. ICP-MS was performed on a Thermo Scientific high resolution inductively-coupled plasma mass spectrometer (HR-ICP-MS) at Texas A&M University's Williams Radiogenic Isotope Geosciences Laboratory for the following nuclides: ^{25}Mg, ^{43}Ca, ^{55}Mn, ^{88}Sr, ^{137}Ba, and ^{56}Fe. The USGS MACS3 coral reference standard was used as a validation standard (N = 12), and error analysis is provided in Table 1. An indium spike was added to all samples and standards to monitor instrumental drift. Because the water samples were not filtered and were acidified for analysis after months in storage, Mn concentrations may be underestimated. Below, we discuss the shell Mn/Ca values without relying heavily on the water measurements.

Cross sections of TP3 and 3R5 shells were photographed with cathodoluminescence microscopy (CL) using a Technosyn 8200 MKII cold cathode luminoscope following the methods of Roark et al. (2016). Samples were exposed to a 400 nA and 20 kV beam with photograph exposure of about 30s. Photomosaics of the CL images were arranged over high resolution scans of the shell cross sections and then analyzed with ImageJ software. Brightness profiles were plotted from the same locations in the shells as the micro-drilled transects. Although some CL photographs had shadows in the bottom left corners, shadows were cropped out in the INL regions. In order to avoid shadows in the VM regions, data points in the shadows were identified on the plot in Figure 3A (corresponding to the labeled regions in Figure 2) and removed from the CL data set analyzed in the cross-

https://doi.org/10.5194/bg-2019-323
Preprint. Discussion started: 30 September 2019

correlation matrix (Table 2). The CL comparisons in Table 2 excluded 8 points from 3R5 and 1 point from TP3 from the shadowy regions of the CL photomosaics. Normalized image brightness profiles were then compared with ICP-MS results using Pearson's *r* values. To avoid false positives with multiple comparisons, we use a Bonferroni correction for the overall level of significance α (0.05), divided by 52 comparisons, resulting in significance threshold of $p < 10^{-3}$.

The distribution coefficient D_{Me} represents the Me/Ca in the shell relative to the water Me/Ca where D_{Me} = (shell Me/Ca) / (water Me/Ca). Ranges of shell D_{Mg}, D_{Mn}, D_{Ba}, and D_{Sr} values were calculated using the minimum and maximum shell Me/Ca values relative to the mean water Me/Ca values for water samples taken from April to August of 2013 to overlap with the growth period of the shell VM trace element data.

3 Results and discussion

3.1 Oxygen isotopes

Stable isotope growth chronologies for specimens 3R5 and TP3 are shown in Figure 3 and explained in detail in VanPlantinga and Grossman (2018). To develop these chronologies, we measured water temperature (T) and $\delta^{18}O_{water}$ to predict shell $\delta^{18}O$ according to equations 1, 2, and 3 (Dettman et al.,1999, based on Grossman and Ku, 1986).

$$1000 \ln(\alpha^{aragonite}_{water}) = 2.559 \times (10^6 \times T^{-2}) + 0.715 \quad (1)$$

$$\alpha^{aragonite}_{water} = \frac{\left(1000+\delta^{18}O_{aragonite_{VPDB}}\right)}{\left(1000+\delta^{18}O_{water_{VSMOW}}\right)} \quad (2)$$

$$\alpha^{VSMOW}_{VPDB} = 1.0309 \text{ (Gonfiantini et al., 1995).} \quad (3)$$

Because winter hiatuses and erratic summer growth patterns result in chaotic shell $\delta^{18}O$ patterns that complicate $\delta^{18}O$ sclerochronology, we used clumped isotope thermometry to supplement $\delta^{18}O$ data (VanPlantinga and Grossman, 2018).

Based on our shell chronology, the time interval represented by the trace element analyses is April to August 2013. During this interval water temperature and $\delta^{18}O_{water}$ ranged from 13 to 34°C and -2.7 to 1.3‰, respectively. Daily average river discharge at the study site was 173-2230 cfs (cubic feet per second; USGS gage

https://doi.org/10.5194/bg-2019-323
Preprint. Discussion started: 30 September 2019

08108700; https://waterdata.usgs.gov). The higher $\delta^{18}O_{water}$ values reflect increased summer evaporation combined with increased proportion of flow from evaporated ^{18}O-enriched Lake Whitney water, whereas lower values (as low as -8‰) are the result of ^{18}O-depleted precipitation and runoff (Chowdhury et al., 2010; VanPlantinga et al., 2017).

3.2 Water chemistry

Mean water Me/Ca values are presented in Table 1. Water dissolved ion concentration and electrical conductivity results are shown in Figure 4A. The Sr, Ca, and Ba results track with the electrical conductivity because Brazos River salinity is strongly controlled by the proportion of river flow discharged from Lake Whitney (Chowdhury et al., 2010; VanPlantinga et al., 2017). Mg, Sr, and Ba correlated positively with Ca concentrations and Mn correlated negatively with Ca (Rsq > 0.55, $p < 0.0007$). Water Mn/Ca, Ba/Ca, and Sr/Ca values (mmol/mol) significantly correlate with each other ($p < 0.00011$), and further, Mg/Ca weakly correlates with Sr/Ca and Ba/Ca ($p < 0.015$). USGS data for the Brazos River gage at Bryan, Texas (08108700) generally display an inverse relationship between dissolved oxygen and discharge. On a linear scale, the element with the highest concentration, calcium, showed the greatest variation (19-83ppm), but on a log scale magnesium concentration showed the most variation (12ppb-20ppm; Figure 4). While the low water manganese concentrations (0.1-0.6 ppb) are consistent with Keeney-Kennicutt and Presley's (1986) measurements (0.1-2.3 ppb), we will not draw conclusions based on the water Mn data because our water samples were not filtered and acidified immediately upon collection. Turekian and Scott (1967) attribute the suspended particulate manganese concentration in the Brazos River (690 ppm) to soil erosion, as found in other river Mn studies (e.g., Shiller, 2002; Risk et al., 2010). The highest water Mn concentration values in our study were from samples taken during times of high flow.

3.3 Shell chemistry

Table 2 explores relationships between environment, growth, and shell chemistry using Pearson's *r* values. Me/Ca values and distribution coefficients (D_{Me}) can differ between specimens 3R5 and TP3, and between the ventral margin (VM) and inner nacreous layer (INL) of the same shell, especially with regard to Mg/Ca and Mn/Ca (Table 1). Nevertheless, taken as a whole, the ranges in values are generally similar to those recorded in previous studies of freshwater mussels (Carroll and Romanek, 2008; Geeza et al., 2018 and references cited therein), except for Mg/Ca (Table 3). In addition, log of shell D_{metal} values overlap with the results in Bolotov et al. (2015) for metal/calcium partitioning in *Margaritifera*, except that their Mg/Ca values are 1-4 orders of magnitude lower than ours (0.001-0.138).

https://doi.org/10.5194/bg-2019-323
Preprint. Discussion started: 30 September 2019

Mg/Ca does not show any systematic patterns in our water data (Figure 3A), nor are there any systematic variations in the Mg/Ca values of the shells, with erratic fluctuations over several orders of magnitude over the time period studied (Figures 4B). Furthermore, taxonomic differences can be important. For example, Mg/Ca values of 3R5 are about three times greater than those of TP3.

Previous studies of Mg/Ca and Sr/Ca indicate that shell trace elements may be heterogeneously distributed in the shell mineral lattice and organic matrix depending on ontogenetic age, ultrastructure, and crystal fabric (Schöne et al., 2011; Schöne et al., 2013). Brazos River water Mg/Ca is about half that in the Scioto River in Ohio (Geeza et al., 2018), but our average shell Mg/Ca values are nearly an order of magnitude higher, resulting in significantly higher D_{Mg} estimates, than in the Ohio *Lamsilis cardium* shells. Differences in species or climate may account for the variation in freshwater mussel D_{Mg} values.

Sr/Ca correlates significantly with Mn/Ca in both shells. If Bonferroni corrections are not used as in other studies (e.g., Vander Putten et al., 2000; Gentry et al., 2008; Izumida et al., 2011; Geeza et al., 2017), all but one Sr/Ca relationship in Table 2 (with growth rate in 3R5) may be significant ($p < 0.05$), corroborating the common observation that Sr/Ca correlates positively with temperature in aragonitic mollusk shells (e.g., Gillikin et al., 2005; Carré et al., 2006; Sosdian et al., 2006). The Sr/Ca-temperature relationship was observed in lacustrine mussels by Izumida et al. (2011), but was not observed in freshwater mussels from Ohio (Geeza et al., 2018) where there was significant shell-water Sr/Ca relationship. The D_{Sr} values from the shell ventral margin regions (0.08-0.19) overlap with D_{Sr} values reported in several previous studies (Carroll and Romanek, 2008; Bolotov et al., 2015; Geeza et al., 2017) as shown in Table 3.

In terms of variation within and between shells, Sr/Ca is only slightly more concentrated in the INL than the VM in both specimens. Figure 4 illustrates the similar patterns between Mn/Ca, CL brightness, shell growth rate, Sr/Ca, and $\delta^{13}C$. There is a robust relationship between Sr/Ca and Mn/Ca in both the TP3 and 3R5 ventral margins (Figure 3E). Sr/Ca values are similar between the two specimens, (Figure 4, Table 1).

As shown in Table 3 shell Ba concentrations in the ventral margin (45-2748 mg/kg) overlap with the range reported in past studies (Carrol and Romanek, 2008; Bolotov et al., 2015; Geeza et al., 2017). Brazos shell D_{Ba} values (0.06-0.47) overlap with values given in other studies of freshwater mussels (Izumida et al., 2011; Bolotov et al., 2015; Geeza et al., 2017). Out of the four Me/Ca parameters, Ba/Ca showed the second lowest mean values in the water and

https://doi.org/10.5194/bg-2019-323
Preprint. Discussion started: 30 September 2019

in the shells. Ba/Ca values overlap with the range reported in past studies (Table 1; Carrol and Romanek, 2008; Bolotov et al., 2015; Geeza et al., 2017). Ba/Ca are 29% higher in the Tampico specimen (TP3) than the threeridge specimen (3R5). Ba/Ca was higher in the Tampico VM region than in the INL, but higher in the threeridge INL than the VM.

While water Ba concentration is likely driven by the proportion of flow from Lake Whitney discharge, as with Sr, Mg, and Ca (Chowdhury et al., 2010; VanPlantinga et al., 2017), the shell Ba/Ca values do not show any systematic patterns. Previous authors have linked shell Ba/Ca to diatom productivity patterns (Vander Putten et al., 2000; Lazareth et al. 2003). In the absence of periodic diatom blooms, Izumida et al. (2011) attributed their lacustrine mussel shell Ba/Ca to growth rate. Our data do not point to a clear physical or physiological explanation for shell Ba/Ca patterns in the Brazos River specimens.

Shell Mn/Ca values (mmol/mol) are shown in Figure 4A. Shell Mn concentrations (67-2308 mg/kg) overlap with ranges reported in several studies (Nyström et al., 1996; Mutvei and Westermark, 2001; Markich et al., 2002; Verdegaal, 2002; Ravera et al., 2003; Langlet et al., 2007; Carroll and Romanek, 2008; Bolotov et al., 2015; Zhao et al., 2017a; Geeza et al., 2017). The D_{Mn} values from the shell ventral margin regions in this study (13-84) overlap with D_{Mn} ranges reported in Geeza et al. (2018) and Bolotov et al. (2015) but are much higher than other studies where $D_{Mn} < 1$ (Markich et al., 2002; Verdegaal, 2002; Carroll and Romanek, 2008). The average D_{Mn} values of the 3R5 and TP3 INL regions are higher (~80-200). Compared to thermodynamic predictions for abiogenic aragonite, biogenic aragonite has relatively high substitution rates of Mn^{2+} for Ca^{2+} in the mineral lattice (Soldati et al., 2016). Relatively high D_{Mn} values (>10) in biogenic aragonite, as reported here, suggest a physiological process of concentrating Mn^{2+} during biomineralization. The influence that factors such as species differences, environment, and ontogeny have on D_{Mn} remain to be determined.

Mn/Ca is significantly higher and more variable in the INL than VM (or ONL) regions in both TP3 and 3R5 specimens (Table 1). Figure 4B shows shell INL Mn/Ca and water Mn/Ca for 2012-2013. Siegele et al. (2001) suggested that shell growth rings have elevated manganese and organic matter content in *Hyridella depressa*, and they inferred different shell chemistry and mineralization processes between the shell umbo and ventral margin. Carroll and Romanek (2008) suggest that differences between INL and ONL trace element values may come from higher rates of dissolution and reprecipitation in the INL than in the ONL. Oeschger (1990) suggested that anaerobiosis

https://doi.org/10.5194/bg-2019-323
Preprint. Discussion started: 30 September 2019

contributes to the internal dissolution of the shell in *Arctica islandica*. Some biomineralization models indicate that the INL is exposed to extrapallial fluid of a different chemical composition than the EPF in contact with the shell ONL region (Schöne and Krause, 2016). If this is the case, then the shell INL trace element values may be less appropriate for environmental reconstruction than the ONL region. Higher Mn/Ca in the INL than in the VM regions of the Brazos River specimens indicates physiological control on the distribution of Mn in the shell. Mn/Ca values are on average 27% higher in the Tampico specimen (TP3) than the threeridge specimen (3R5). This may reflect species or individual differences in metabolic rate.

Shell Mn/Ca correlates inversely with log of river discharge (Table 2), allowing for the reconstruction of times of high and low flow. Figure 3F reconstructs trends in log of Brazos River discharge ($\log_{10}Q$) from Mn/Ca in TP3 ($\log_{10}Q = -1.11 \times Mn/Ca_{shell} + 3.17$) and in 3R5 ($\log_{10}Q = -1.22 \times Mn/Ca_{shell} + 2.99$). The reconstruction is more accurate in the summer but overestimates observed discharge in the spring, possibly due to seasonal changes in water Mn/Ca or biological controls on shell Mn/Ca. Because of 1) the higher Mn/Ca in the INL relative to the VM regions in the shells, and 2) the strong relationship between shell Mn/Ca and river discharge, we infer both physical and biological controls on shell Mn/Ca, as discussed below.

Previous studies have used shells chemistry to reconstruct river discharge such as by linking high runoff events to elevated suspended Mn from soil erosion (Risk et al., 2010). Many sclerochronological reconstructions of discharge are based on stable oxygen isotopes (Mueller-Lupp et al., 2003; Dettman et al., 2004; Versteegh et al., 2011; Ricken et al., 2003; Kelemen et al., 2018). Our study indicates that Brazos River mussel activity patterns (feeding and/or metabolic rate) are influenced by discharge rates and that these variations are recorded in the trace element composition, particularly Mn/Ca, of the shell mineral. Here we reconstruct river discharge variation and distinguish times of low and high flow using shell Mn/Ca values (Figure 3F).

3.4 Cathodoluminescence

Cathodoluminescence (CL) is a common tool for mapping the distribution of manganese in biogenic carbonates (Barbin, 2000). Lattice-bound Mn caused greenish-yellow luminescence under CL. The CL images reveal alternating bright green-yellow and dim banding that generally correlates with the pattern of light and dark banding in plane light (Figure 2). The results verify that the Mn is lattice-bound (Table 2) and reveal the complex

https://doi.org/10.5194/bg-2019-323
Preprint. Discussion started: 30 September 2019

cyclicity of Mn distribution in the shell (Lartaud et al., 2009). CL brightness also weakly correlates with Sr/Ca and G (growth rate) in both shells.

3.5 Dissolved and particulate sources of Mn

Manganese incorporated into the mussel shells may be derived from dissolved Mn or ingested particulate Mn. Several factors affect manganese concentration and flux in the environment. Reducing conditions, low DO, and low pH increase manganese solubility (Tebo et al., 2004). Microbial activity combined with high nutrient flux and low rates of water column mixing can cause hypoxia, reducing conditions, and elevated dissolved Mn^{2+} concentration (Zhao et al., 2017a). Other factors influencing Mn availability include photo-inhibition of Mn^{2+}-oxidizing bacteria, reductive dissolution from sunlight (Sunda and Huntsman, 1994), primary production, benthic decomposition, algal uptake of dissolved Mn^{2+} (Sunda and Huntsman, 1985), and influx of allochthonous dissolved Mn^{2+} (Langlet et al., 2007).

Shell manganese could be influenced by point sources such Lake Whitney or the Little River. Lake Whitney and Little River manganese concentrations are near the mean values of the Brazos River (~0.2ppb; this study). Lake Whitney has periodic brown algae blooms (Roelke et al., 2011). However, if Lake Whitney was the driver of shell Mn/Ca patterns, then the water Mn/Ca patterns would not be inversely related to water Sr/Ca, Ba/Ca, and Mg/Ca. Elevated $\delta^{13}C$ in the shells during the summer of 2013 was interpreted as an indication of heightened Lake Whitney influence on river flow and chemistry during drought conditions (VanPlantinga and Grossman, 2018; VanPlantinga et al., 2017). There is a correlation between $\delta^{13}C$ and Mn/Ca in 3R5 but not in TP3. There is not yet sufficient evidence to indicate that Lake Whitney or the Little River are point sources of shell manganese, nor to explain the striking inverse shell Mn/Ca - river discharge relationship, but the point source hypothesis cannot be ruled out given the important role Lake Whitney plays in downstream river chemistry (VanPlantinga et al., 2017).

Dissolved Mn^{2+} is the most bioavailable form of manganese (Campbell, 1995). Shell Mn/Ca values have been attributed to variations in dissolved Mn^{2+} in the water column (Frietas et al., 2006; Barats et al., 2008) and in the sediment porewater (Zhao et al., 2017a). As mentioned earlier, experimental studies have confirmed that dissolved Mn^{2+} content is recorded in shell Mn/Ca (Jeffree et al., 1995; Hawkes et al., 1996; Markich et al., 2002; Langlet et al., 2006; Lartaud et al., 2010). However, the low dissolved oxygen conditions in the Brazos River, which should favor high dissolved Mn^{2+}, occur at times of high flow (USGS 08108700 gage data) when shell Mn/Ca is

https://doi.org/10.5194/bg-2019-323
Preprint. Discussion started: 30 September 2019

relatively low. Redox conditions in the water column do not explain the shell Mn/Ca patterns, and we lack the data to evaluate the hypothesis that sediment porewater drives shell Mn/Ca.

Particulate Mn, bound to organic or inorganic particles, can also be a source of Mn in shells. The inverse relationship between water Ca and Mn concentrations indicates that Mn flux into the water may be related to runoff from local rain storms, in contrast to the Ca sourced from the upstream reservoir Lake Whitney (Chowdhury et al., 2010; VanPlantinga et al., 2017). Bilos et al. (1998) attributed elevated clam soft tissue Mn to higher turbidity and ingestion of Mn-bearing inorganic particles. Because Mn/Ca is inversely correlated with log of discharge in this study, inorganic particles (suspended during at times of high flow) are probably not the source of Brazos River mussel shell Mn/Ca.

Previous studies have attributed bivalve shell Mn/Ca to ingestion of Mn-bearing organic particles such as phytoplankton. Vander Putten et al. (2000) and Lazareth et al. (2003) found significant shell Ba/Ca-Mn/Ca correlations in estuarine bivalves indicative of diatom ingestion. Brazos River phytoplankton are typically not diatoms (Roelke, personal communication) and there is no shell Ba/Ca-Mn/Ca relationship in our data. Geeza et al. (2018) examined oxygen, chlorophyll, and pH as a proxy for primary productivity (based on Goodwin et al., 2018), but did not find correlations with shell Mn/Ca. Nevertheless, they could not rule out a phytoplankton or microbial manganese reduction (Lovley and Phillips, 1988) influences on their shell Mn/Ca values.

Roach et al. (2014) found elevated chlorophyll concentrations in the Brazos River near our study site at times of low discharge in 2010-2012, with suspended chlorophyll concentration significantly higher than benthic chlorophyll (40-50 mg/L compared to ~11 mg/L), and about 5-10 times higher than the other rivers in their study. Roach (2013) attributed river chlorophyll abundance to lengthened residence time, emphasizing that sediment scouring and turbidity from high discharge limit phytoplankton growth (Wissmar et al. 1981; Steinman and McIntire, 1990). River mussels have been observed to preferentially inhabit refugia with low rates of shear stress (Layzer and Madison, 1995; Strayer, 1999; Howard and Cuffey, 2003). This may correspond to elevated manganese concentrations in sediment porewater as in Zhao et al. (2017a). However, little is known about the spatial and temporal variation and chemical composition of Brazos River phytoplankton, suspended load, and colloids in the flowing river water and the sediment porewater. Future work should characterize these variables.

3.6 Manganese accumulation in shells

https://doi.org/10.5194/bg-2019-323
Preprint. Discussion started: 30 September 2019

Shell Mn/Ca is potentially determined by a combination of environmental chemistry (e.g., water and particle chemistry), physical conditions (e.g., temperature and discharge), and the behavior of the organism (e.g., feeding rate, growth rate, and reproductive investment). Zhao et al. (2017b) offer a similar interpretation of *Corbicula fluminea* shell Ba/Ca based on laboratory experiments. In terms of feeding behavior, mussels selectively ingest organic matter during filter feeding (Hawkins et al., 1996). Zhao et al. (2017a) propose that manganese bioaccumulation in lacustrine mussels is enhanced by deposit feeding (Vaughn and Hakenkamp, 2001; Cahoon and Owen, 1996). The elevated concentrations of suspended chlorophyll relative to benthic chlorophyll at our study location at times of low flow are conditions favorable for suspension feeding (Roach et al., 2014). The propensity in river mussels to inhabit refugia with minimal shear stress (Layzer and Madison, 1995; Strayer, 1999; Howard and Cuffey, 2003) supports the hypothesis that Brazos River mussels thrive under conditions of low discharge with high concentrations of suspended particulate organic matter to feed on.

It is important to consider the physiological processes and soft tissues potentially involved in manganese bioaccumulation. Langlet et al. (2007) suggest that soft tissues concentrate Mn derived from the digestion and absorption of organic particles and this may lead to elevated Mn/Ca values in the shells. Acidic pH in the gut makes ingested particulate Mn bioavailable so that it can then accumulate in mollusk soft tissue and the shell (Arifin and Bendell-Young, 2000; Owen, 1996). Nott and Nicolaidou (1993) found that a substantial 67% of ingested manganese is not recovered in feces of the mollusk *Nussarius rericulatus*, and therefore it is absorbed through the digestive tract. Mollusk bioaccumulation of heavy metals through the gills and digestive glands is well documented and supports the hypothesis that shell manganese can bioaccumulate via food ingestion (Domouhtsidou et al., 2000; Dimitriadis et al., 2003; Einsporn and Koehler, 2008).

The shell Sr/Ca-Mn/Ca may indicate a relationship between metabolic rate, inferred from Sr/Ca, and feeding rate, inferred from Mn/Ca. Metabolic rate is influenced by factors such as ontogeny, reproductive investment, environmental stress (drought, flood, predation), and seasonal feeding patterns (Bayne et al., 1989). Brazos mussel shell Sr/Ca may reflect metabolic patterns that cause varying rates of ion transport into the EPF as hypothesized in Carré et al. (2006). Zhao et al. (2016) experimentally changed dissolved Ca^{2+} concentrations and used lanthanum and Verapamil to artificially inhibit Ca^{2+} channels in the freshwater bivalve *Corbicula fluminea* and concluded that Mn^{2+} and Ca^{2+} compete to cross ion channels during biomineralization. In light of the important role ion channels play in

https://doi.org/10.5194/bg-2019-323
Preprint. Discussion started: 30 September 2019

biomineralization, the Sr/Ca-Mn/Ca correlation in the Brazos River shells points to a relationship between metabolic rate and feeding rate. However, the physiological mechanism of ion channels does not diminish the importance of environmental factors such as water chemistry and redox conditions in determining shell Me/Ca values, as indicated in many studies (Campbell, 1995; Jeffree et al., 1995; Hawkes et al., 1996; Markich et al., 2000; Frietas et al., 2006; Langlet et al., 2006; Barats et al., 2008; Lartaud et al., 2010; Zhao et al., 2017a; and for Sr/Ca in the case of Geeza et al., 2017).

Little is known about the pathway that environmental manganese takes from ingestion to shell mineralization. Amorphous calcium carbonate (ACC), conveyed by hemocytes to the mantle, is the precursor to the shell mineral (Addadi et al., 2003; Mount et al., 2004; Li et al., 2016). The ACC has higher Mn and other metal concentrations than the shell mineral (Thomson et al., 1985; Jacob et al., 2008). Initial manganese exposure may be primarily to the gills, hemolymph, mantle, or digestive tract, and it may travel to the site of biomineralization via particulate or dissolved forms through the hemolymph and mantle tissue. Marin et al. (2012) describe intercellular and intracellular dissolution and formation of ACC granules in the mantle tissue, potentially blurring the distinction between granule and calcium ion channel transport of trace metals to be incorporated into the shell mineral lattice. Dissolved and ACC-bound Mn^{2+} physiological pathways should be investigated further.

5 Conclusions

Mn/Ca values for Brazos River mussel shells showed a cyclical pattern revealed by time series analyses and cathodoluminescence, which maps a pattern similar to the growth bands. Mn/Ca correlated inversely with discharge, allowing for a reconstruction of river discharge patterns during the study period. Mn/Ca is likely influenced by ingestion rates of Mn-bearing suspended particulate organic matter because shell Mn/Ca is high when river discharge and turbidity are low, ruling out inorganic particles as the control on shell Mn/Ca. The shell Mn-Sr relationship and the evidence of high suspended chlorophyll at times of low flow (Roach et al., 2014) point to elevated metabolic activity and likely increased feeding rate in response to food abundance, and possibly lower shear stress and turbidity, at times of low flow. Future research on shell and water chemistry should: 1) further the scientific understanding of river plankton, suspended colloidal and sediment porewater manganese variation; 2) resolve taxonomic D_{Mn} differences; and 3) elucidate specifically why different mussels in different environments have D_{Mn} values <1 and others D_{Mn} values are >10.

https://doi.org/10.5194/bg-2019-323
Preprint. Discussion started: 30 September 2019

Code/Data Availability

Data are available on earthchem.org.

Authors' Contributions

A. VanPlantinga collected and analyzed data, made plots and tables, and wrote and revised the manuscript. E. Grossman provided funding and edited the manuscript, the plots, and the tables.

Competing Interests

The authors have no competing interests to declare.

Acknowledgments

The authors would like to thank the Michel T. Halbouty Chair in Geology at Texas A&M University for supporting this research. Luz Romero, Franco Marcantonio, and the Texas A&M AgriLife Extension Soil, Water and Forage Testing Laboratory analyzed shell and/or water samples. Charles Randklev and Eric Tsakiris collected the mussel specimens. Ann Molineux from The University of Texas Jackson School Museum of Earth History provided historical specimens from the Singley-Askew Collection. Charles Randklev and Robert G. Howells provided helpful perspective on mussel ecology. Ben Passey, Naomi Levin, Huanting Hu, Haoyuan Ji, Sophie Lehmann, Dana Brenner, and Lai Ming provided valuable assistance at the Johns Hopkins University Stable Isotope Lab. Chris Maupin, Lauren Graniero, Andrew Roark, and Brendan Roark helped run isotope samples at the Stable Isotope Geoscience Facility at Texas A&M University. Clumped isotope analyses were financed by NSF grant EAR-1226918. Data reported here are in the following online repository: earthchem.org. We thank reviewers Christopher Romanek and David Dettman for their helpful comments.

References

Addadi, L., Raz, S. and Weiner, S.: Taking advantage of disorder: amorphous calcium carbonate and its roles in biomineralization. *Advanced Materials*, *15*(12), pp.959–970, 2003.

Arifin, Z. and Bendell-Young, L.I.: Influence of a selective feeding behaviour by the blue mussel *Mytilus trossulus* on the assimilation of 109Cd from environmentally relevant seston matrices. *Marine Ecology Progress Series*, *192*, pp.181–193, 2000.

https://doi.org/10.5194/bg-2019-323
Preprint. Discussion started: 30 September 2019

Barats, A., Amouroux, D., Pécheyran, C., Chauvaud, L. and Donard, O.F.X.: High-frequency archives of manganese inputs to coastal waters (Bay of Seine, France) resolved by the LA-ICP-MS analysis of calcitic growth layers along scallop shells (*Pecten maximus*). *Environmental Science & Technology*, *42*(1), pp.86–92, 2007.

Barbin, V.: Cathodoluminescence of carbonate shells: biochemical vs diagenetic process, in *Cathodoluminescence in Geosciences*, edited, pp. 303–329, Springer, 2000.

Bayne, B.L., Hawkins, A.J.S., Navarro, E. and Iglesias, I.P.: Effects of seston concentration on feeding, digestion and growth in the mussel Mytilus edulis. *Marine Ecology Progress Series*, pp.47–54, 1989.

Bellotto, V.R. and Miekeley, N.: Trace metals in mussel shells and corresponding soft tissue samples: a validation experiment for the use of Perna perna shells in pollution monitoring. *Analytical and Bioanalytical Chemistry*, *389*(3), pp.769–776, 2007.

Bilos, C., Colombo, J.C. and Presa, M.J.: Trace metals in suspended particles, sediments and Asiatic clams (*Corbicula fluminea*) of the Río de la Plata Estuary, Argentina. *Environmental Pollution*, *99*(1), pp.1–11, 1998.

Bolotov, I.N., Pokrovsky, O.S., Auda, Y., Bespalaya, J.V., Vikhrev, I.V., Gofarov, M.Y., Lyubas, A.A., Viers, J. and Zouiten, C.: Trace element composition of freshwater pearl mussels *Margaritifera* spp. across Eurasia: testing the effect of species and geographic location. *Chemical Geology*, *402*, pp.125–139, 2015.

Carré, M., Bentaleb, I., Bruguier, O., Ordinola, E., Barrett, N.T. and Fontugne, M.: Calcification rate influence on trace element concentrations in aragonitic bivalve shells: evidences and mechanisms. *Geochimica et Cosmochimica Acta*, *70*(19), pp.4906–4920, 2006.

Carroll, M., and Romanek, C. S.: Shell layer variation in trace element concentration for the freshwater bivalve *Elliptio complanata*, *Geo-Marine Letters*, *28*(5-6), 369–381, doi:10.1007/s00367-008-0117-3, 2008.

Chale, F.M.M.: Trace metal concentrations in water, sediments and fish tissue from Lake Tanganyika. *Science of the Total Environment*, *299*(1–3), pp.115–121, 2002.

Chowdhury A, Osting T, Furnans J, Mathews R.: Groundwater–surface water interaction in the Brazos River Basin: evidence from lake connection history and chemical and isotopic compositions: Texas Water Development Board Report, 375 (August):1–61, 2010.

Dettman, D. L., and Lohmann, K. C.: Microsampling carbonates for stable isotope and minor element analysis: Physical separation of samples on a 20 micrometer scale: *Journal of Sedimentary Research*, *65*(3), 1995.

Dettman, D. L., Reische, A. K. and Lohmann, K.C.: Controls on the stable isotope composition of seasonal growth bands in aragonitic fresh-water bivalves (Unionidae), *Geochimica et Cosmochimica Acta*, *63*(7), 1049–1057, 1999.

Dettman, D. L., K. W. Flessa, P. D. Roopnarine, B. R. Schöne, and Goodwin, D. H.: The use of oxygen isotope variation in shells of estuarine mollusks as a quantitative record of seasonal and annual Colorado River discharge, *Geochimica et Cosmochimica Acta*, *68*(6), 1253–1263, 2004.

Dimitriadis, V.K., Domouhtsidou, G.P. and Raftopoulou, E.: Localization of Hg and Pb in the palps, the digestive gland and the gills in *Mytilus galloprovincialis* (L.) using autometallography and X-ray microanalysis. *Environmental Pollution*, *125*(3), pp.345–353, 2003.

Domouhtsidou, G.P. and Dimitriadis, V.K.: Ultrastructural localization of heavy metals (Hg, Ag, Pb, and Cu) in gills and digestive gland of mussels, *Mytilus galloprovincialis* (L.). *Archives of Environmental Contamination and Toxicology*, *38*(4), pp.472–478, 2000.

https://doi.org/10.5194/bg-2019-323
Preprint. Discussion started: 30 September 2019

Einsporn, S. and Koehler, A., 2008. Immuno-localisations (GSSP) of subcellular accumulation sites of phenanthrene, aroclor 1254 and lead (Pb) in relation to cytopathologies in the gills and digestive gland of the mussel *Mytilus edulis*. *Marine environmental research*, *66*(1), pp.185–186.

Freitas, P.S., Clarke, L.J., Kennedy, H., Richardson, C.A. and Abrantes, F.: Environmental and biological controls on elemental (Mg/Ca, Sr/Ca and Mn/Ca) ratios in shells of the king scallop *Pecten maximus*. *Geochimica et Cosmochimica Acta*, *70*(20), pp.5119–5133, 2006.

Geeza, T.J., Gillikin, D.P., Goodwin, D.H., Evans, S.D., Watters, T. and Warner, N.R.: Controls on magnesium, manganese, strontium, and barium concentrations recorded in freshwater mussel shells from Ohio, *Chemical Geology*, 2018.

Gentry, D.K., Sosdian, S., Grossman, E.L., Rosenthal, Y., Hicks, D. and Lear, C.H.: Stable isotope and Sr/Ca profiles from the marine gastropod *Conus ermineus*: testing a multiproxy approach for inferring paleotemperature and paleosalinity. *Palaios*, *23*(4), pp.195–209, 2008.

Gillikin, D.P., Lorrain, A., Navez, J., Taylor, J.W., André, L., Keppens, E., Baeyens, W. and Dehairs, F.: Strong biological controls on Sr/Ca ratios in aragonitic marine bivalve shells. *Geochemistry, Geophysics, Geosystems*, *6*(5), 2005.

Hawkes, G., Day, R., Wallace, M., Nugent, K., Bettiol, A., Jamieson, D. and Williams, M.: Analyzing the growth and form of mollusc shell layers, in situ, by cathodoluminescence microscopy and Raman spectroscopy, *Journal of Shellfish Research*, *15*(3), 659–666, 1996.

Howard, J.K. and Cuffey, K.M., 2003. Freshwater mussels in a California North Coast Range river: occurrence, distribution, and controls. *Journal of the North American Benthological Society*, *22*(1), pp.63–77.

Immenhauser, A., Schoene, B.R., Hoffmann, R. and Niedermayr, A.: Mollusc and brachiopod skeletal hard parts: intricate archives of their marine environment. *Sedimentology*, *63*(1), pp.1–59, 2016.

Jacob, D.E., Soldati, A.L., Wirth, R., Huth, J., Wehrmeister, U. and Hofmeister, W., 2008. Nanostructure, composition and mechanisms of bivalve shell growth. *Geochimica et Cosmochimica Acta*, *72*(22), pp.5401–5415.

Jeffree, R.A., Markich, S.J., Lefebvre, F., Thellier, M. and Ripoll, C.: Shell microlaminations of the freshwater bivalve *Hyridella depressa* as an archival monitor of manganese water concentration: Experimental investigation by depth profiling using secondary ion mass spectrometry (SIMS). *Experientia*, *51*(8), pp.838–848, 1995.

Keeney-Kennicutt, W.L. and Presley, B.J.: The geochemistry of trace metals in the Brazos River estuary. *Estuarine, Coastal and Shelf Science*, *22*(4), pp.459–477, 1986.

Kelemen, Z., Gillikin, D.P. and Bouillon, S.: Relationship between river water chemistry and shell chemistry of two tropical African freshwater bivalve species. *Chemical Geology*, 2018.

Langlet, D., Alleman, L.Y., Plisnier, P.D., Hughes, H. and André, L.: Manganese content records seasonal upwelling in Lake Tanganyika mussels. *Biogeosciences*, *4*(2), pp.195–203, 2007.

Lartaud, F., De Rafélis, M., Ropert, M., Emmanuel, L., Geairon, P. and Renard, M.: Mn labelling of living oysters: artificial and natural cathodoluminescence analyses as a tool for age and growth rate determination of *C. gigas* (Thunberg, 1793) shells. *Aquaculture*, *300*(1–4), pp.206–217, 2010.

Layzer, J B. and Madison, L.M., Microhabitat use by freshwater mussels and recommendations for determining their instream flow needs. Regulated Rivers: Research and Management 10:329–345, 1995.

Lazareth, C.E., Vander Putten, E., André, L. and Dehairs, F.: High-resolution trace element profiles in shells of the mangrove bivalve *Isognomon ephippium*: a record of environmental spatio-temporal variations?. *Estuarine, Coastal and Shelf Science*, *57*(5–6), pp.1103–1114, 2003.

https://doi.org/10.5194/bg-2019-323
Preprint. Discussion started: 30 September 2019

Li, S., Liu, Y., Liu, C., Huang, J., Zheng, G., Xie, L. and Zhang, R.: Hemocytes participate in calcium carbonate crystal formation, transportation and shell regeneration in the pearl oyster *Pinctada fucata*. *Fish & Shellfish Immunology*, *51*, pp.263–270, 2016.

Lovley, D.R., Phillips, E.J.: Novel mode of microbial energy metabolism: organic carbon oxidation coupled to dissimilatory reduction of iron or manganese. *Appl. Environ. Microbiol. 54* (6), 1472–1480, 1988.

Lydeard, C., Cowie, R.H., Ponder, W.F., Bogan, A.E., Bouchet, P., Clark, S.A., Cummings, K.S., Frest, T.J., Gargominy, O.and Herbert, D.G.: The global decline of nonmarine mollusks, *BioScience*, *54*(4), 321–330, 2004.

Markich, S.J., Jeffree, R.A. and Burke, P.T.: Freshwater bivalve shells as archival indicators of metal pollution from a copper-uranium mine in tropical northern Australia. *Environ. Sci. Technol. 36*, 821–832, 2002.

Marin, F., Le Roy, N. and Marie, B.: The formation and mineralization of mollusk shell. *Front Biosci*, *4*(1099), p.125, 2012.

Mount, A.S., Wheeler, A.P., Paradkar, R.P. and Snider, D.: Hemocyte-mediated shell mineralization in the eastern oyster. *Science*, *304*(5668), pp.297–300, 2004.

Müller-Lupp, T., Erlenkeuser, H. and Bauch, H.: Seasonal and interannual variability of Siberian river discharge in the Laptev Sea inferred from stable isotopes in modern bivalves. *Boreas*, *32*(2), pp.292–303, 2003.

Mutvei, H., Westermark, T.: How environmental information can be obtained from Naiad shells. *Ecol. Evol. freshw. mussels Unionoida 145*, 367–379, 2001.

Nielsen-Gammon, J.W.: The changing climate of Texas, in *The impact of global warming on Texas. University of Texas Press, Austin*, edited, pp. 39–68, 2011.

Nott, J.A. and Nicolaidou, A.: Bioreduction of zinc and manganese along a molluscan food chain. *Comparative Biochemistry and Physiology Part A: Physiology*, *104*(2), pp.235–238, 1993.

Nyström, J., Dunca, E., Mutvel, H., Lindh, U.: Environmental history as reflected by freshwater pearl mussels in the River Vramsån, southern Sweden. *Ambio 25* (5), 350–355, 1996.

Oeschger, R.: Long-term anaerobiosis in sublittoral marine invertebrates from the Western Baltic Sea: *Halicryptus spinulosus (Priapulida)*, *Astarte borealis* and *Arctica islandica (Bivalvia*). *Marine Ecology Progress Series*, pp.133–143, 1990.

Puente, X., Villares, R., Carral, E. and Carballeira, A.: Nacreous shell of *Mytilus galloprovincialis* as a biomonitor of heavy metal pollution in Galiza (NW Spain). *Science of the Total Environment*, *183*(3), pp.205–211, 1996.

Randklev, C.R., Johnson, M.S., Tsakiris, E.T., Groce, J. and Wilkins, N.: Status of the freshwater mussel (*Unionidae*) communities of the mainstem of the Leon River, Texas, *Aquatic Conservation: Marine and Freshwater Ecosystems*, *23*(3), 390–404, doi:10.1002/aqc.2340, 2013.

Ravera, O., Cenci, R., Beone, G.M., Dantas, M. and Lodigiani, P.: Trace element concentrations in freshwater mussels and macrophytes as related to those in their environment, *Journal of Limnology*, *62*(1), 61–70, 2003.

Richter, B.D., Braun, D.P., Mendelson, M.A. and Master, L.L.: Threats to imperiled freshwater fauna, *Conservation Biology*, *11*(5), 1081–1093, 1997.

https://doi.org/10.5194/bg-2019-323
Preprint. Discussion started: 30 September 2019

Ricken, W., Steuber, T., Freitag, H., Hirschfeld, M. and Niedenzu, B.: Recent and historical discharge of a large European river system–oxygen isotopic composition of river water and skeletal aragonite of *Unionidae* in the Rhine. *Palaeogeography, Palaeoclimatology, Palaeoecology*, *193*(1), pp.73–86, 2003.

Risk, M.J., Burchell, M., De Roo, K., Nairn, R., Tubrett, M. and Forsterra, G.: Trace elements in bivalve shells from the Río Cruces, Chile. *Aquatic Biology*, *10*(1), pp.85–97, 2010.

Roach, K.A.: Environmental factors affecting incorporation of terrestrial material into large river food webs. *Freshwater Science*, *32*(1), pp.283–298, 2013.

Roach, K.A., Winemiller, K.O. and Davis III, S.E.: Autochthonous production in shallow littoral zones of five floodplain rivers: effects of flow, turbidity and nutrients. *Freshwater Biology*, *59*(6), pp.1278–1293, 2014.

Roark, A., Grossman, E.L. and Lebold, J.: Seasonality and circulation dynamics along the Appalachian margin of the Late Pennsylvanian epicontinental sea of North America: brachiopod geochemical records and their implications to models of shelf anoxia. *Geological Society of America Bulletin*, *128*, 597–608, 2016.

Roelke, D.L., Grover, J.P., Brooks, B.W., Glass, J., Buzan, D., Southard, G.M., Fries, L., Gable, G.M., Schwierzke-Wade, L., Byrd, M. and Nelson, J.: A decade of fish-killing *Prymnesium parvum* blooms in Texas: roles of inflow and salinity. *Journal of Plankton Research*, *33*(2), 2011.

Schöne, B.R., Zhang, Z., Radermacher, P., Thébault, J., Jacob, D.E., Nunn, E.V. and Maurer, A.F.: Sr/Ca and Mg/Ca ratios of ontogenetically old, long-lived bivalve shells (*Arctica islandica*) and their function as paleotemperature proxies. *Palaeogeography, Palaeoclimatology, Palaeoecology*, *302*(1–2), pp.52–64, 2011.

Schöne, B.R., Radermacher, P., Zhang, Z. and Jacob, D.E.: Crystal fabrics and element impurities (Sr/Ca, Mg/Ca, and Ba/Ca) in shells of *Arctica islandica*—Implications for paleoclimate reconstructions. *Palaeogeography, Palaeoclimatology, Palaeoecology*, *373*, pp.50–59, 2013.

Schöne, B.R. and Krause Jr, R.A.: Retrospective environmental biomonitoring–Mussel Watch expanded. *Global and Planetary Change*, *144*, pp.228–251, 2016.

Shiller, A.M.: Seasonality of dissolved rare earth elements in the lower Mississippi River. Geochemistry, Geophysics, Geosystems 3(11): 1068, 2002.

Siegele, R., Orlic, I., Cohen, D.D., Markich, S.J. and Jeffree, R.A.: Manganese profiles in freshwater mussel shells. *Nuclear Instruments and Methods in Physics Research Section B: Beam Interactions with Materials and Atoms*, *181*(1–4), pp.593–597, 2001.

Silva, C.A.R., Smith, B.D. and Rainbow, P.S.: Comparative biomonitors of coastal trace metal contamination in tropical South America (N. Brazil). *Marine Environmental Research*, *61*(4), pp.439–455, 2006.

Soldati, A.L., Jacob, D.E., Glatzel, P., Swarbrick, J.C. and Geck, J.: Element substitution by living organisms: the case of manganese in mollusc shell aragonite. *Scientific reports*, *6*, p.22514, 2016.

Sosdian, S., Gentry, D.K., Lear, C.H., Grossman, E.L., Hicks, D. and Rosenthal, Y.: Strontium to calcium ratios in the marine gastropod *Conus ermineus*: Growth rate effects and temperature calibration. *Geochemistry, Geophysics, Geosystems*, *7*(11), 2006.

Steinman, A.D. and McIntire, C.D.: Recovery of lotic periphyton communities after disturbance. *Environmental Management*, *14*(5), pp.589–604, 1990.

Strayer, D.L.: Use of flow refuges by unionid mussels in rivers. *Journal of the North American Benthological Society*, *18*(4), pp.468–476, 1999.

Sunda, W.G. and Huntsman, S.A.: Regulation of cellular manganese and manganese transport rates in the unicellular alga Chlamydomonas1. *Limnology and oceanography*, *30*(1), pp.71–80, 1985.

https://doi.org/10.5194/bg-2019-323
Preprint. Discussion started: 30 September 2019

Sunda, W.G. and Huntsman, S.A.: Diel cycles in microbial manganese oxidation and manganese redox speciation in coastal waters of the Bahama Islands. *Limnology and Oceanography*, *35*(2), pp.325–338, 1990.

Sunda, W.G. and Huntsman, S.A.: Photoreduction of manganese oxides in seawater. *Marine Chemistry*, *46*(1–2), pp.133–152, 1994.

Tebo, B.M., Bargar, J.R., Clement, B.G., Dick, G.J., Murray, K.J., Parker, D., Verity, R. and Webb, S.M.: Biogenic manganese oxides: properties and mechanisms of formation. *Annu. Rev. Earth Planet. Sci.*, *32*, pp.287–328, 2004.

Thomson, J.D., Pirie, B.J. and George, S.G.: Cellular metal distribution in the Pacific oyster, *Crassostrea gigas* (Thun.) determined by quantitative X-ray microprobe analysis. *Journal of experimental marine biology and ecology*, *85*(1), pp.37–45, 1985.

Trimmer, M., Grey, J., Heppell, C.M., Hildrew, A.G., Lansdown, K., Stahl, H. and Yvon-Durocher, G.: River bed carbon and nitrogen cycling: state of play and some new directions. *Science of the total environment*, *434*, pp.143–158, 2012.

Tsakiris, E.T. and Randklev, C.R.: Structural changes in freshwater mussel (*Bivalvia: Unionidae*) assemblages downstream of Lake Somerville, Texas. *The American Midland Naturalist*, *175*(1), pp.120–128, 2016.

Turekian, K.K. and Scott, M.R.: Concentrations of chromium, silver, molybdenum, nickel, cobalt, and manganese in suspended material in streams. *Environmental science & technology*, *1*(11), pp.940–942, 1967.

Vander Putten, E., Dehairs, F., Keppens, E. and Baeyens, W.: High resolution distribution of trace elements in the calcite shell layer of modern *Mytilus edulis*: Environmental and biological controls. *Geochimica et Cosmochimica Acta*, *64*(6), pp.997–1011, 2000.

VanPlantinga, A.A., Grossman, E.L. and Roark, E.B.: Chemical and isotopic tracer evaluation of water mixing and evaporation in a dammed Texas river during drought. *River Research and Applications*, *33*(3), pp.450–460, 2017.

VanPlantinga, A.A. and Grossman, E.L.: Stable and clumped isotope sclerochronologies of mussels from the Brazos River, Texas (USA): Environmental and ecologic proxy. *Chemical Geology*, *502*, pp.55–65, 2018.

Vaughn, C.C. and Hakenkamp, C.C.: The functional role of burrowing bivalves in freshwater ecosystems. *Freshwater Biology*, *46*(11), pp.1431–1446, 2001.

Verdegaal, S.: The shell chemistry of *Unio crassus batavus* as tool for reconstructing the evolution of the Rhine–Meuse delta and its use as indicator for river water composition. *Vrije Universiteit, Amsterdam*, 2002.

Versteegh, E.A., Vonhof, H.B., Troelstra, S.R. and Kroon, D.: Can shells of freshwater mussels (*Unionidae*) be used to estimate low summer discharge of rivers and associated droughts?. *International Journal of Earth Sciences*, *100*(6), pp.1423–1432, 2011.

Wheeler, A.P.: Mechanisms of molluscan shell formation. *Calcification in biological systems*, pp.179–216, 1992.

Wissmar, R.C., Richey, J.E., Stallard, R.F. and Edmond, J.M.: Plankton metabolism and carbon processes in the Amazon River, its tributaries, and floodplain waters, Peru–Brazil, May–June 1977. *Ecology*, *62*(6), pp.1622–1633, 1981.

Zeng, F.W., Masiello, C.A. and Hockaday, W.C.: Controls on the origin and cycling of riverine dissolved inorganic carbon in the Brazos River, Texas. *Biogeochemistry*, *104*(1–3), pp.275–291, 2011.

Zhao, L., Schöne, B.R. and Mertz-Kraus, R.:. Delineating the role of calcium in shell formation and elemental composition of *Corbicula fluminea* (Bivalvia). *Hydrobiologia*, *1*(790), pp.259–272, 2016.

Zhao, L., Walliser, E.O., Mertz-Kraus, R. and Schöne, B.R.: Unionid shells (*Hyriopsis cumingii*) record manganese cycling at the sediment–water interface in a shallow eutrophic lake in China (Lake Taihu). *Palaeogeography, Palaeoclimatology, Palaeoecology*, *484*, pp.97–108, 2017a.

https://doi.org/10.5194/bg-2019-323
Preprint. Discussion started: 30 September 2019

Zhao, L., Schöne, B.R. and Mertz-Kraus, R.: Controls on strontium and barium incorporation into freshwater bivalve shells (*Corbicula fluminea*). *Palaeogeography, palaeoclimatology, palaeoecology*, *465*, pp.386–394, 2017b.

https://doi.org/10.5194/bg-2019-323
Preprint. Discussion started: 30 September 2019

Biogeosciences
Discussions
Open Access

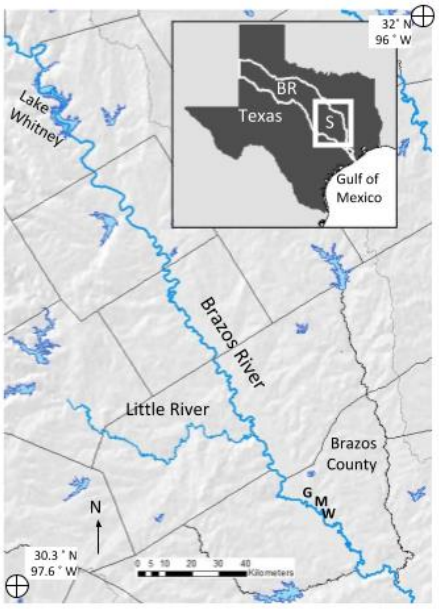

Figure 1. Study area. Inset: Map of Texas, Brazos River watershed (BR), and study area (S). The map reaches from Lake Whitney in the north to Brazos County in the south, showing the water collection (W), mussel collection (M), and gage (G, USGS gage 08108700) locations.

625

https://doi.org/10.5194/bg-2019-323
Preprint. Discussion started: 30 September 2019

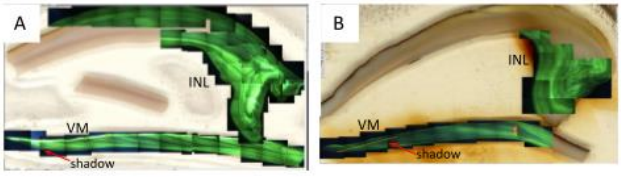

Figure 2. Cathodoluminescence (CL) photomosaics for TP3 (A), 3R5 (B). Thin yellow lines in A and B are the transects analyzed with ImageJ. The sampled INL (inner nacreous layer) and VM (ventral margin) regions are labeled in A and B.

626

https://doi.org/10.5194/bg-2019-323
Preprint. Discussion started: 30 September 2019

Biogeosciences
Discussions
Open Access

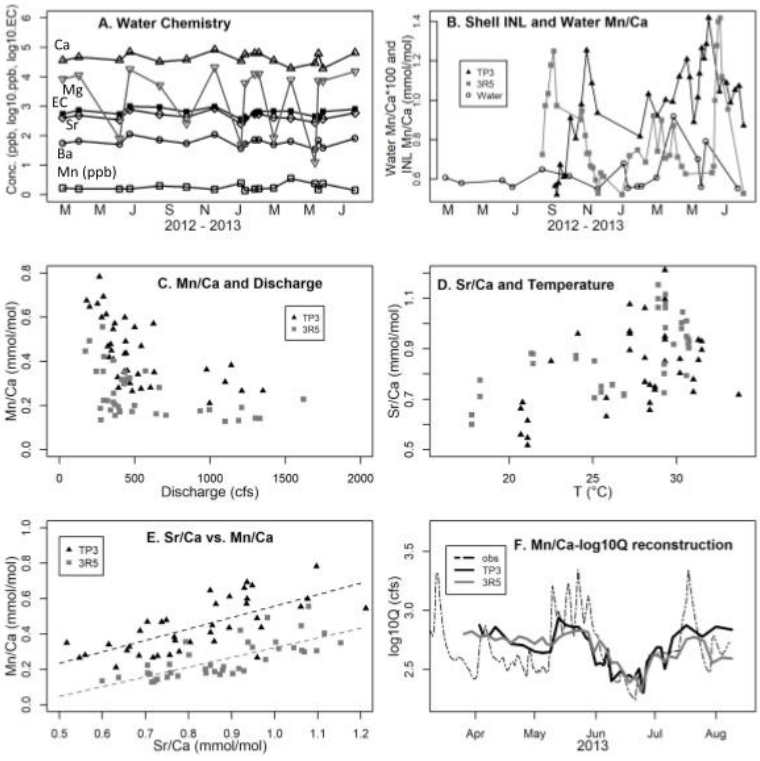

Figure 3. (A) Water chemistry measurements from the Brazos River (2012-2013); empty squares = Mn (ppb), empty circles = Ba (log10 of ppb), empty upright triangles = Ca (log10 of ppb), filled squares = electrical conductivity (log10 of µS), inverted empty triangles = Mg (log10 of ppb), diamonds = Sr (log10 of ppb). (B) Water Mn/Ca (100*mmol/mol) and shell INL Mn/Ca in mmol/mol. (C) Discharge vs. Mn/Ca. (D) Temperature vs. Sr/Ca. (E) Shell Sr/Ca vs. shell Mn/Ca values. (F) Log10 of river discharge (Q) and reconstructions of log10 (Q) based on the shell Mn/Ca-Q relationship.

627

https://doi.org/10.5194/bg-2019-323
Preprint. Discussion started: 30 September 2019

Biogeosciences
Discussions
Open Access
EGU

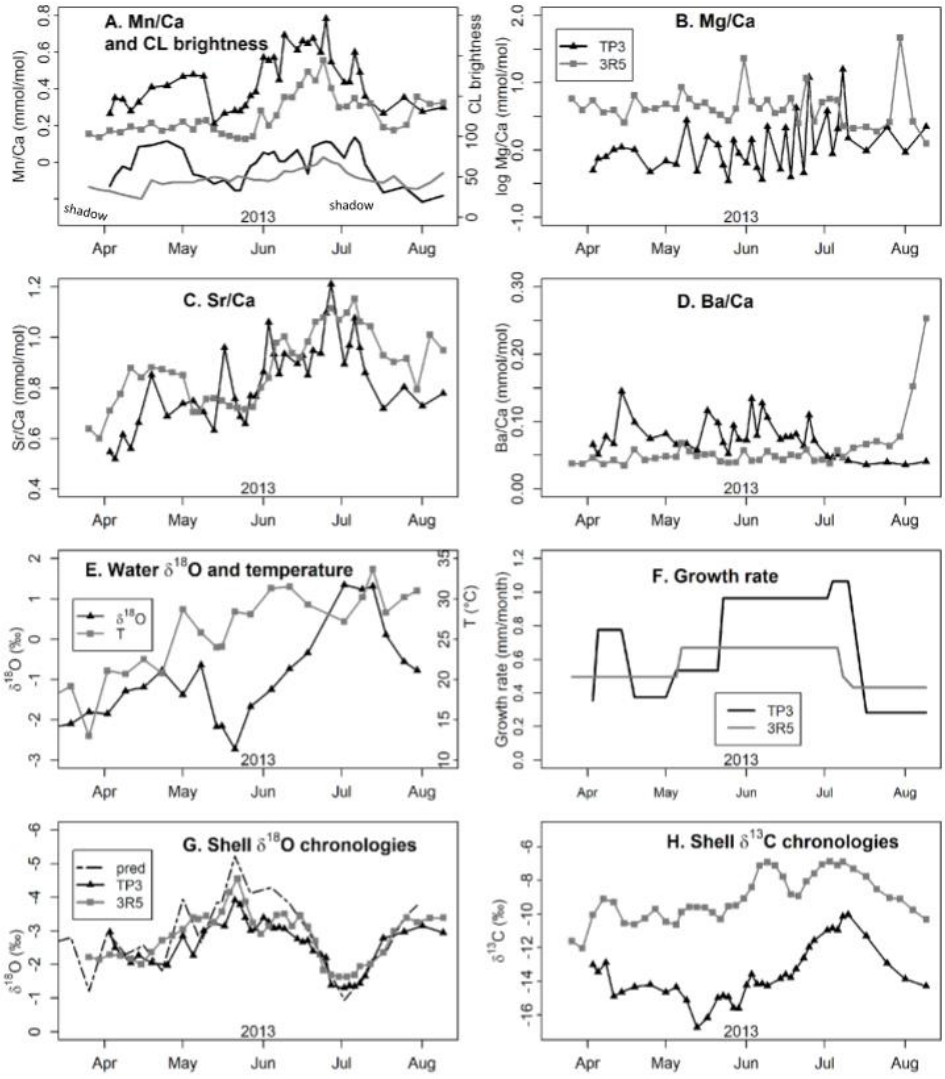

Figure 4. TP3 (black triangles and/or black line), and 3R5 (gray squares and/or gray line) values for shell Mn/Ca and CL (A); shell Mg/Ca (B); shell Sr/Ca (C); shell Ba/Ca (D); water $\delta^{18}O$ and temperature (E); estimated shell growth rate (F); shell $\delta^{18}O$ chronologies for TP3, 3R5, and predicted aragonite $\delta^{18}O$ (G); and shell $\delta^{13}C$ chronologies (H). The shell isotope chronologies are described in detail in Van Plantinga and Grossman (2018).

628

https://doi.org/10.5194/bg-2019-323
Preprint. Discussion started: 30 September 2019

Biogeosciences Discussions
Open Access
EGU

Table 1. Summary of MACS3 check standard results and error analysis and Brazos River water and shell results by shell region for trace metal Me/Ca values and calculated partition coefficients D(Me/Ca of shell/water).

	Mn/Ca	Sr/Ca	Ba/Ca	Mg/Ca
MACS3 check standard and uncertainty analysis				
Mean*	1.07	8.70	0.05	7.70
Std. dev.*	0.082	0.187	0.004	0.151
RSD	7.6%	2.2%	7.6%	2.0%
Precision	2.2%	0.6%	2.2%	0.6%
Accuracy	3.5%	0.7%	6.5%	3.9%
Cert. values*	1.11	8.76	0.05	8.01
*mmol/mol Ca				
Mean Brazos River and mussel shell values (mmol/mol Ca)				
Water	0.006	5.45	0.46	292.9
TR5VM	0.26	0.88	0.058	6.86
TR5INL	0.83	1.13	0.085	0.79
TP3VM	0.44	0.82	0.072	2.07
TP3INL	1.29	1.05	0.058	13.63
Mean distribution coefficients				
TR5VM	27	0.14	0.11	0.02
TR5INL	89	0.18	0.16	0.002
TP3VM	47	0.13	0.14	0.006
TP3INL	135	0.16	0.11	0.04

https://doi.org/10.5194/bg-2019-323
Preprint. Discussion started: 30 September 2019

Table 2. r^2 and p values for relationships between log10 of discharge (log Q), temperature (T), river water $\delta^{18}O_w$, growth rate (G in mm/month), $\delta^{18}O$, $\delta^{13}C$, Mn/Ca, Sr/Ca and CL for specimens TP3 and 3R5. R^2 and p values are in **bold** if p is less than the Bonferroni-corrected α value of 0.05 / 52 = 0.001. Gray italicized p values exceed the Bonferroni-corrected α value.

	CL R^2	CL p	Mn R^2	Mn p	Sr R^2	Sr p	G R^2	G p	$\delta^{18}O$ R^2	$\delta^{18}O$ p
TP3										
log Q	**0.31**	**3.7E-04**	**0.49**	**1.6E-06**	0.13	2.6E-02	*0.02*	*4.2E-01*	0.20	6.1E-03
T	*0.00*	*7.4E-01*	0.18	9.8E-03	0.26	1.2E-03	*0.06*	*1.4E-01*	*0.04*	*2.1E-01*
$\delta^{18}O_w$	0.13	3.0E-02	*0.07*	*1.0E-01*	0.18	8.4E-03			**0.56**	**1.2E-07**
G	0.26	1.4E-03	**0.27**	**9.5E-04**	0.24	2.3E-03				
$\delta^{18}O$			*0.06*	*1.6E-01*	0.12	3.7E-02				
$\delta^{13}C$	0.14	2.5E-02	*0.09*	*7.4E-02*	0.20	5.9E-03	*0.10*	*5.6E-02*		
CL			**0.43**	**1.2E-05**	**0.34**	**1.7E-04**				
Sr/Ca			**0.49**	**1.5E-06**						
3R5										
log Q	0.16	2.1E-02	**0.45**	**2.3E-05**	0.29	1.6E-03	*0.00*	*9.1E-01*	*0.12*	*5.6E-02*
T	0.18	1.5E-02	0.27	2.3E-03	0.30	1.2E-03	*0.00*	*7.4E-01*	*0.03*	*3.1E-01*
$\delta^{18}O_w$	*0.02*	*4.6E-01*	0.17	2.0E-02	**0.53**	**2.0E-06**			**0.65**	**2.6E-08**
G	0.21	8.4E-03	*0.04*	*2.9E-01*	*0.01*	*6.4E-01*				
$\delta^{18}O$			0.22	7.3E-03	**0.58**	**4.9E-07**				
$\delta^{13}C$	0.20	1.1E-02	0.25	3.2E-03	**0.53**	**2.7E-06**	*0.06*	*1.8E-01*		
CL			**0.61**	**1.6E-07**	0.31	1.0E-03				
Sr/Ca			**0.56**	**7.6E-07**						

https://doi.org/10.5194/bg-2019-323
Preprint. Discussion started: 30 September 2019

Biogeosciences
Discussions
Open Access
EGU

Table 3. Comparison of shell chemistry and shell/water distribution coefficient results (D_{Me}) with past studies (based on Geeza et al., 2017).

Reference	Sr (mg/kg)	D_{Sr}	Ba (mg/kg)	D_{Ba}	Mg (mg/kg)	D_{Mg} ($\times 10^{-3}$)	Mn (mg/kg)	D_{Mn}	Dissolved Mn
Faure et al. (1967)		0.22–0.28							
Nyström et al. (1996)	300–600						10–600		
Mutvei and Westermark (2001)							400–6000		
Markich et al. (2002)							300–1700	0.6	
Verdegaal (2002)	120–220		0.1				100–700	0.5	
Bailey and Lear (2006)	700–1000	0.28							
Langlet et al. (2007)							100–1000		
Ravera et al. (2007)							200–800		
Carroll and Romanek (2008)	120–2000	0.17–0.26	60–400	0.05			80–1700	0.2–0.5	36–188
Izumida et al. (2011)		0.18–0.22		0.069–0.086	150–500	0.30–0.42			
Bolotov et al. (2015)	345–595	0.15–0.26	32–92	0.2–0.6	23–43	0.2–0.4	139–469	10–300	
Zhao et al. (2017)	1130–1380						400–1800		70–1400
Geeza et al. (2017)	820–3343	0.16–0.20	15–270	0.11–0.14	26–1200	0.3–0.8	120–1250	32–42	10–60
This study	430–5279	0.08–0.19	45–2748	0.06–0.47	36–89718	1–138	67–2308	13–84	0.1–0.6
Water Data	Sr		Ba		Mg		Mn		
Water Conc. (ppb), this study	255–852		34–112		12–20837		0.1–0.6		
Water Me/Ca (mmol/mol)	3–10		0.2–1.0		0.7–714.9		0.001–0.022		

631